Dual-arm robotic manipulation of flexible cables

Jihong Zhu, Benjamin Navarro, Philippe Fraisse, André Crosnier and Andrea Cherubini

Flexible cables (e.g., power cables, HDMI cables etc) are commonly used in industrial/household environment. These cables deform under force acting on them. Humans can manipulate cables using two hands. Given a (reachable) desired cable shape, a human is able to deform the cable into the target shape. Such task is easy for a human to do without knowing the internal dynamics of the cable (see Fig. 1). For the robot, it still remains a challenge.

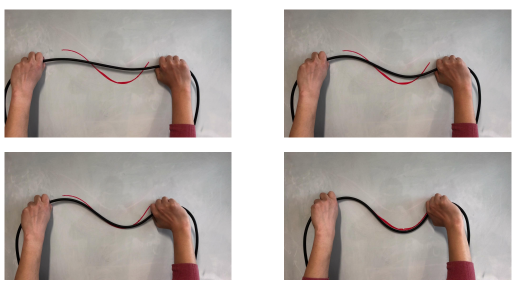

Fig. 1: Cable manipulation by humans, red color lines mark the desired shape

In the literatures, there exist some works on manipulation of flexible cables. Nakagaki et al. and Zheng [1], [2] focused on the cable insertion task. These approaches all utilized a deformation model of the flexible object and considered only the single arm. Kosuge et al. [3] studied dual arm manipulation of a flexible beam using a finite element model. Recently, Navarro-Alarcon et al. proposed several model-free methods for manipulation of flexible objects [4], [5], [6], [7].

We draw inspiration from [7], and extend the work to dual arm manipulation of an open contour, such as the shape of a flexible cable. The objective of this work is to enable a dual-arm robot to complete the task of deforming a flexible cable to a desired shape through vision-based control without prior knowledge of the deformation model.

A. Problem formulation

A dual-arm robot is used to manipulate a cable on a 2D plane. The cable can be regarded as a system with unknown dynamics that accepts inputs from the robot. There are in total 6 inputs from the robot:

$$\boldsymbol{r} = [\dot{x}_1 \;\; \dot{y}_1 \;\; \omega_1 \;\; \dot{x}_2 \;\; \dot{y}_2 \;\; \omega_2]^T \in \mathbb{R}^6. \tag{1}$$

Each of the end-effectors applies 3 velocity inputs, respectively: two translation velocities in the manipulation plane, $\dot{x}$ and $\dot{y}$, and one angular velocity ω along the axis perpendicular to the manipulation plane.

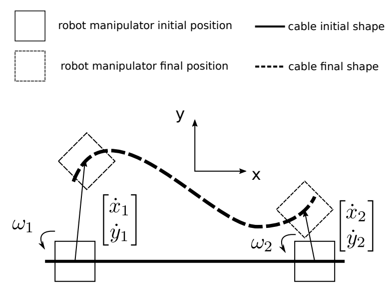

Fig. 2: Control inputs

The shape of the cable is continuously observed by a static camera perpendicular to the manipulation plane. The cable shape on the camera image is represented as $\boldsymbol{c} = [\boldsymbol{u}, \boldsymbol{v}]^T$, where $\boldsymbol{u}$ and $\boldsymbol{v}$ are image coordinates of pixels sampled along the cable. We represent the desired cable shape by $\boldsymbol{c}^*$.

The problem is to use the control inputs $\boldsymbol{r}$ to drive the cable from its initial shape $\boldsymbol{c}_0$ to the desired shape $\boldsymbol{c}^*$ with on-line estimated deformation model by visual feedback.

B. Feature parameters

Assume there are in total K samples of image coordinates in $\boldsymbol{c}$. The i^{th} sample $c(i) = [u(i), v(i)]^T$, $i = 1, 2, \ldots, K$ can be approximated using Fourier series:

$$\begin{aligned} u(i) &= \sum_{j=1}^{N} [a_j \;\; b_j] \begin{bmatrix} cos(j\rho_i) \\ sin(j\rho_i) \end{bmatrix} + e \\ v(i) &= \sum_{j=1}^{N} [c_j \;\; d_j] \begin{bmatrix} cos(j\rho_i) \\ sin(j\rho_i) \end{bmatrix} + f, \end{aligned} \tag{2}$$

with

$$\rho_i = (i-1)\frac{\pi}{K}, \tag{3}$$

$N \geq 1$ is the order of the Fourier series.

We denote $\boldsymbol{s}$ to be the feature parameters characterize (2):

$$\boldsymbol{s} = [a_1 \; b_1 \; \ldots \; a_N \; b_N \; e \; c_1 \; d_1 \; \ldots \; c_N \; d_N \; f]^T \in \mathbb{R}^{4N+2}. \tag{4}$$

It will later be used in deformation model estimation and control. We will show how we solve for $\boldsymbol{s}$ given image data.

We can rewrite (2) as:

$$c(i) = \begin{bmatrix} u(i) \\ v(i) \end{bmatrix} = \begin{bmatrix} \boldsymbol{F}(i) & \boldsymbol{0} \\ \boldsymbol{0} & \boldsymbol{F}(i) \end{bmatrix} \boldsymbol{s}. \tag{5}$$

In (5), $\boldsymbol{F}(i)$ are the harmonics terms defined as:

$$\boldsymbol{F}(i) = [\cos\rho_i \;\; \sin\rho_i \;\; \ldots \;\; \cos(N\rho_i) \;\; \sin(N\rho_i) \;\; 1] \in \mathbb{R}^{2N+1}, \tag{6}$$

The authours are with the Laboratory for Computer Science, Microelectronics and Robotics LIRMM - Université de Montpellier CNRS, 161 Rue Ada, 34090 Montpellier, France. firstname.lastname@lirmm.fr

Using all K samples in $\boldsymbol{c}$, we have:

$$\boldsymbol{c} = \boldsymbol{G}\boldsymbol{s}, \tag{7}$$

with:

$$\boldsymbol{c} = [c(1)^T \ c(2)^T \ \ldots \ c(K)^T]^T \in \mathbb{R}^{2K},$$

$$\boldsymbol{G} = \begin{bmatrix} \boldsymbol{F}(1) & \boldsymbol{0} \\ \boldsymbol{0} & \boldsymbol{F}(1) \\ \vdots & \vdots \\ \boldsymbol{F}(K) & \boldsymbol{0} \\ \boldsymbol{0} & \boldsymbol{F}(K) \end{bmatrix} \in \mathbb{R}^{2K\times(4N+2)}. \tag{8}$$

Feature parameters of the shape can be solved by linear least squares:

$$\boldsymbol{s} = (\boldsymbol{G}^T\boldsymbol{G})^{-1}\boldsymbol{G}^T\boldsymbol{c}, \tag{9}$$

C. Local deformation model estimation

The feature parameters $\boldsymbol{s}$ describes the cable shape. A small movement of the robot will produce a tiny change in the cable shape, hence on the feature parameters. From this observation, at a given operating point, we are able to linearize the deformation model as:

$$\delta\boldsymbol{s} = \boldsymbol{Q}\delta\boldsymbol{r}. \tag{10}$$

In (10)

$$\delta\boldsymbol{r} = \boldsymbol{r}\delta t \in \mathbb{R}^6, \tag{11}$$

corresponds to the change in robot position with δt being the time interval and $\boldsymbol{r}$ being the velocity inputs of the robot; $\delta\boldsymbol{s} \in \mathbb{R}^{4N+2}$ is the change in feature parameters, and $\boldsymbol{Q} \in \mathbb{R}^{(4N+2)\times 6}$ is the local deformation matrix relating the two.

For the i^{th} element of $\boldsymbol{s}$, we can write:

$$\delta s_i = \delta\boldsymbol{r}^T\boldsymbol{q}_i, \tag{12}$$

where $\boldsymbol{q}_i^T \in \mathbb{R}^6$ is the i^{th} row of $\boldsymbol{Q}$.

To estimate $\boldsymbol{q}_i$, we denote the current time as t_m. Using a constant sampling period δt, within the time period $(m-1)\delta t$, we collect m consecutive data of δs_i and $\delta\boldsymbol{r}^T$ while the robot is moving:

$$\boldsymbol{\sigma}_i = \begin{bmatrix} \delta s_i(t_1) \\ \delta s_i(t_2) \\ \vdots \\ \delta s_i(t_m) \end{bmatrix} \in \mathbb{R}^m, \boldsymbol{R} = \begin{bmatrix} \delta\boldsymbol{r}^T(t_1) \\ \delta\boldsymbol{r}^T(t_2) \\ \vdots \\ \delta\boldsymbol{r}^T(t_m) \end{bmatrix} \in \mathbb{R}^{m\times 6}, \tag{13}$$

where

$$t_k = t_m - (m-k)\delta t, \ \ k = 1,2,3,\ldots,m. \tag{14}$$

Using $\boldsymbol{R}$ and $\boldsymbol{\sigma}_i$ we have:

$$\boldsymbol{\sigma}_i = \boldsymbol{R}\boldsymbol{q}_i. \tag{15}$$

Then, $\boldsymbol{q}_i$ can be estimated via:

$$\hat{\boldsymbol{q}}_i = (\boldsymbol{R}^T\boldsymbol{R})^{-1}\boldsymbol{R}^T\boldsymbol{\sigma}_i. \tag{16}$$

D. Shape servo controller

The differences between the initial shape $\boldsymbol{c}$ and the desire shape $\boldsymbol{c}_d$ can be characterized by the difference between Fourier coefficients of two shapes:

$$\Delta\boldsymbol{s} = \boldsymbol{s} - \boldsymbol{s}_d. \tag{17}$$

Using the estimated deformation model:

$$\delta\boldsymbol{s} = \hat{\boldsymbol{Q}}\delta\boldsymbol{r}. \tag{18}$$

We can use the servo control law from [7]:

$$\delta\boldsymbol{r} = -\lambda(\hat{\boldsymbol{Q}}^T\hat{\boldsymbol{Q}})^{-1}\hat{\boldsymbol{Q}}^T\,\mathrm{sat}(\Delta\boldsymbol{s}) \tag{19}$$

where λ is a feedback gain and $\mathrm{sat}(\cdot)$ is a vectorial saturation function.

E. Experimental setup and result

The cable is attached to both end-effectors. A camera is placed perpendicular to the manipulation plane to track the shape of the cable during manipulation.

Figure 3 depicts one experiment. The red color line is the target shape. In each figure, the initial and final shape of the cable is presented in (a) and (d) respectively. Figure (b) and (c) shows the intermediate shapes while reaching the final shape.

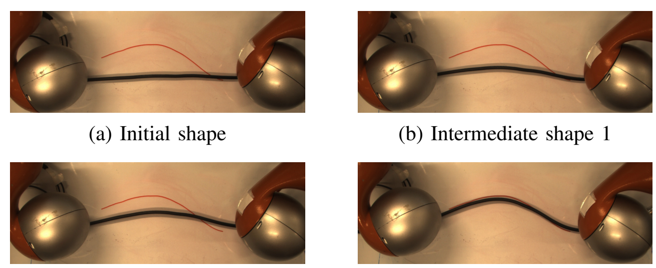

(a) Initial shape (b) Intermediate shape 1

(c) Intermediate shape 2 (d) Final shape

Fig. 3: Robot experiment

References

[1] H. Nakagaki, K. Kitagaki, T. Ogasawara, and H. Tsukune, “Study of deformation and insertion tasks of a flexible wire,” in *IEEE Int. Conf. on Robotics and Automation*, vol. 3, 1997, pp. 2397–2402.

[2] Y. F. Zheng, R. Pei, and C. Chen, “Strategies for automatic assembly of deformable objects,” in *IEEE Int. Conf. on Robotics and Automation*. IEEE, 1991, pp. 2598–2603.

[3] K. Kosuge, H. Yoshida, T. Fukuda, M. Sakai, and K. Kanitani, “Manipulation of a flexible object by dual manipulators,” in *IEEE Int. Conf. on Robotics and Automation*, vol. 1, 1995, pp. 318–323.

[4] D. Navarro-Alarcon, Y. Liu, J. G. Romero, and P. Li, “Model-free visually servoed deformation control of elastic objects by robot manipulators,” *IEEE Trans. on Robotics*, vol. 29, no. 6, pp. 1457–1468, 2013.

[5] D. Navarro-Alarcon and Y. Liu, “Uncalibrated vision-based deformation control of compliant objects with online estimation of the jacobian matrix,” in *IEEE/RSJ Int. Conf. on Intelligent Robots and Systems*, 2013, pp. 4977–4982.

[6] D. Navarro-Alarcon, Y. Liu, J. G. Romero, and P. Li, “On the visual deformation servoing of compliant objects: Uncalibrated control methods and experiments,” *Int. Journal of Robotics Research*, vol. 33, no. 11, pp. 1462–1480, 2014.

[7] D. Navarro-Alarcon and Y.-H. Liu, “Fourier-based shape servoing: A new feedback method to actively deform soft objects into desired 2-D image contours,” *IEEE Trans. on Robotics*, 2017.